Carbohydrate Polymers 83 (2011) 414–421

Contents lists available at ScienceDirect

Carbohydrate Polymers

journal homepage: www.elsevier.com/locate/carbpol

Thermal, rheological, mechanical and morphological behavior of HDPE/chitosan blend

Sadullah Mir[a,b,c], Tariq Yasin[b,*], Peter J. Halley[c], Humaira Masood Siddiqi[a], Timothy Nicholson[c]

[a] Department of Chemistry, Quaid-i-Azam University, Islamabad 45320, Pakistan
[b] Department of Chemical and Materials Engineering, Pakistan Institute of Engineering and Applied Sciences, Nilore, Islamabad, Pakistan
[c] Centre for High Performance Polymers, Division of Chemical Engineering, The University of Queensland, Brisbane, Qld 4072, Australia

ARTICLE INFO

Article history:
Received 19 November 2009
Received in revised form 28 July 2010
Accepted 30 July 2010
Available online 7 August 2010

Keywords:
Chitosan
HDPE
Rheology
Silane
Crosslinking

ABSTRACT

A peroxide-initiated melt compounding technique was used to graft and crosslink the high density polyethylene/chitosan blend using vinyl triethoxysilane. Different percentage of chitosan (up to maximum of 35%) was added in HDPE/chitosan blends. The physical and functional properties of the crosslinked HDPE/chitosan blends were investigated and compared with its non-crosslinked congener. IR spectrum of crosslinked blend confirmed the presence of Si–O–Si and Si–O–C absorption peaks at 1020 cm^{-1} and 1105 cm^{-1}. Increased gel content was obtained with increasing chitosan loading whereas percentage crystallinity was decreased. Rheological study of crosslinked blends showed linear viscoelastic behavior with high complex viscosity and dynamic shear storage modulus. Tensile strength of crosslinked HDPE was 9.3 MPa and it was increased by threefold to 27.4 MPa in crosslinked HDPE/chitosan blends containing 35% chitosan contents. Similarly lower deformation was observed in crosslinked blends under static load. Scanning electron microscopy revealed good adhesion between matrix–filler interphase.

1. Introduction

Polyolefins have many applications in our daily life and their consumption is continuously increasing. These materials are extensively used in high volume for short term applications such as packaging film, healthcare, construction, automobile, agricultural, etc. and are disposed off at dump sites as waste. These polymers are very resistant to degradation and their complete degradation takes several years and the environment suffers long term pollution (Orhan, Hrenovic, & Buyukgungor, 2004). Recycling of polymeric waste is a better solution for this problem but it is very costly. Moreover, the recycled products have poor qualities (Tzankova & Lamantia, 1999). Major research is going on to make these material degradable and environment friendly.

Many synthetic biodegradable polymers such as polylactic acid (Constance, Chu, & Monosov, 1995) and polycaprolactone (Maria, Mariola, & Helena, 1998) were developed and commercialized but they were very expensive with limited shelf life. Alternatively, polymer blends and composites containing natural polymers as biodegradable additives (such as starch, cellulose and their derivatives) were developed (Alain & Sylvie, 2008; Jung & Junseok, 2009; Otey, Westhoff, & Doane, 1980; Tae & Hiroshi, 1980). These composites are easily extrudable and commercialized. The major disadvantage of incorporating natural polymer into synthetic polymer is their compatibility. Natural polymers are hydrophilic while synthetic polymers are hydrophobic in nature. The resultant blend of these two types of polymers is almost immiscible. The poor interaction between matrix and filler interphase causes weaker mechanical properties (Magnus, Paul, & Kristiina, 2005). In order to improve interaction, modification of both the polymer and additives has been made (Araujo, Waldman, & De Paoli, 2008; Girones et al., 2007; Hongdian, Yuan, Ming, Zuyao, & Weicheng, 2006; Valenza, Visco, & Acierno, 2002).

In this work, effort has been made to develop a polyolefin blend containing natural polymer with improved mechanical properties. A film grade high density polyethylene (HDPE) has been selected and blended with chitosan which is a natural polymer and it gives two advantages. It acts as a biodegradable additive and gives antimicrobial properties to the blend (Zivanovic, Li, Davidson, & Kit, 2007). It has been reported in literature that highly deacetylated chitosan is more antimicrobial than acetylated chitosan (Sekiguchi, 1994). In fact it is the amino group which controls the antimicrobial activity of the chitosan. Vinyl triethyoxysilane (VTES) has been selected as a crosslinking agent because it has good binding ability both for HDPE and chitosan. Different weight percentage of HDPE and chitosan were used to prepare blends. The thermal, mechanical, rheological and morphological properties of the blends were investigated and compared with its non-crosslinked congener.

* Corresponding author. Tel.: +92 51 2207380–82; fax: +92 51 2208070.
E-mail address: yasintariq@yahoo.com (T. Yasin).

0144-8617/$ – see front matter © 2010 Elsevier Ltd. All rights reserved.
doi:10.1016/j.carbpol.2010.07.069

2. Experimental

2.1. Materials

HDPE with melt flow index of 2.2 g/10 min (190 °C/2.16 kg) was purchased from Sigma–Aldrich Australia. Chitosan (from crab shells, ≥75% deacetylated), vinyl triethoxysilane (VTES), dicumyl peroxide (DCP), dibutyltin dilaurate (DBTDL) and stearic acid were also supplied by Sigma–Aldrich Australia. All the chemicals were used without further purification.

2.2. Sample preparation

The chitosan was dried in vacuum oven for 24 h at 80 °C. The moisture content of chitosan was measured using Sartorius moisture analyzer. The moisture content before and after drying the chitosan was 13.7% and 3.1% respectively. After drying, the chitosan was cryogrinded into fine powder using Cryo-grinder (8650 Freeze/Mill). The particle's size distribution of chitosan was then determined by Malvern Instrument (Mastersizer 2000) using water as dispersant.

A series of HDPE/chitosan blends with weight ratio of 100/0, 85/15, 75/25, 70/30, 65/35 were prepared using Brabender internal mixer at 170 °C with rotor speed of 40 rpm. For crosslinked blends, following steps were taken. In all crosslinked formulations, fixed amounts of DCP (0.15 phr, part per hundred parts of resin) and DBTDL (0.05 phr) were dissolved in dry acetone and were sprayed over HDPE pellets. In order to remove acetone the HDPE pellets were dried at 60 °C in oven for 5 min. The DCP coated HDPE pellets were mixed with chitosan and stearic acid (0.3 phr) in internal mixer for 3 min at (T = 130 °C, rotor speed = 33 rpm). Fixed amount of VTES (2.8 phr) was gradually added to the mixture during melting stage. For the next 7 min, the temperature and the rotor speed were fixed at 170 °C and 40 rpm respectively. Finally, the blended material was heat pressed into sheets at 170 °C under 50 kN load. The prepared sheets were crosslinked in hot water at 90 ± 1 °C for 20 h. After crosslinking, the sheets were dried in vacuum oven for 16 h at 70 °C.

2.3. Structural analysis

The structure analysis of the blends was examined by Fourier transform infrared spectroscopy (FTIR). The IR spectra of the films were recorded by FTIR spectrophotometer (Thermo Electron Corporation, Nicolet 6700) using attenuated total reflection technique. The spectrum was scanned from 4000 cm^{-1} to 500 cm^{-1} at the resolution of 6 cm^{-1}. An average of 32 scans was recorded.

2.4. Gel content

The gel contents of the prepared samples were determined according to ASTM 2765. The samples were crushed into fine pieces, placed into copper cloth and weighed. Extraction was carried out with *p*-xylene for 15 h in Soxhlet extractor. The extracted specimens were washed with acetone and then dried to a constant weight under vacuum. The gel contents of the specimens were calculated using the following equation.

$$\text{Gel content (\%)} = \frac{\text{weight after extraction}}{\text{weight of original specimen} - \text{weight of chitosan}} \times 100$$

2.5. Thermogravimetric analysis

The thermal stability of the samples was studied by using thermogravimetric analysis. These experiments were performed on a Mettler Toledo (TGA/DSC star system), under nitrogen flow of 50 mL/min. Approximately 8–10 mg of sample was placed in the alumina pan at a heating rate of 10 °C/min from room temperature to 550 °C.

2.6. Differential scanning calorimetry

Differential scanning calorimetry (DSC) of the blended material was performed using DSC Q2000 instrument. The samples were cut into small pieces and ~5 mg of each sample was used for analysis. To remove the thermal history, the sample was heated from 25 °C to 180 °C and cooled to −50 °C and then reheated up to 180 °C at a heating rate of 10 °C/min under nitrogen atmosphere.

2.7. Rheological analysis

The time and temperature dependent storage modulus (G'), loss modulus (G'') and complex viscosity (η^*) were determined by Advance Rheometric Expansion System (ARES) using parallel plate geometry having plate diameter of 25 mm. The specimens from the compression molded sheets were cut according to the diameter of the plate. The experiment was performed at 150 °C over the frequency range of 0.05–100 rad/s. The gap between the plates was automatically adjusted by the instrument.

2.8. Tensile properties

The tensile properties were determined using an Instron tensile tester (model 5543). The instrument was operated at a crosshead speed of 50 mm min^{-1} using 5-kN static load cell. The specimens were cut into dumb bell shape (Dimension; Type 4, Standard; ISO 37:1994) from a 1-mm thick compression molded sheet. Five specimens from each sample were tested.

2.9. Creep test

The creep experiments were performed using DMTA IV (Rheometric Scientific). The instrument was operated in tensile mode at 60 °C. The dimensions of the specimens were 1.4 mm × 6 mm × 25 mm. The constant static stress of 2 MPa was applied for 5 h. Five specimens from each sample were tested.

2.10. Morphological analysis

Scanning electron microscope (Jeol, JSM, 6400F) was used to study the morphology of the prepared samples. Specimens were dried overnight in vacuum oven and then freeze fractured. Carbon fibers were used to coat the fractured surfaces. The instrument was operated at 10–15 kV. Energy dispersive spectroscopy (EDS) was used to determine the elemental composition of the specimens.

3. Results and discussion

3.1. Mechanism of silane crosslinking

A series of crosslinked HDPE/chitosan blends were prepared by melt compounding technique and crosslinked with VTES in the presence of dicumyl peroxide. The proposed mechanism of various reactions that occur during processing and silane crosslinking is shown in Scheme 1 [i (a–d)]. DCP dissociates into peroxy radicals at higher temperature and these radicals attack on polyethylene and chitosan chains. This reaction generates free radicals on the

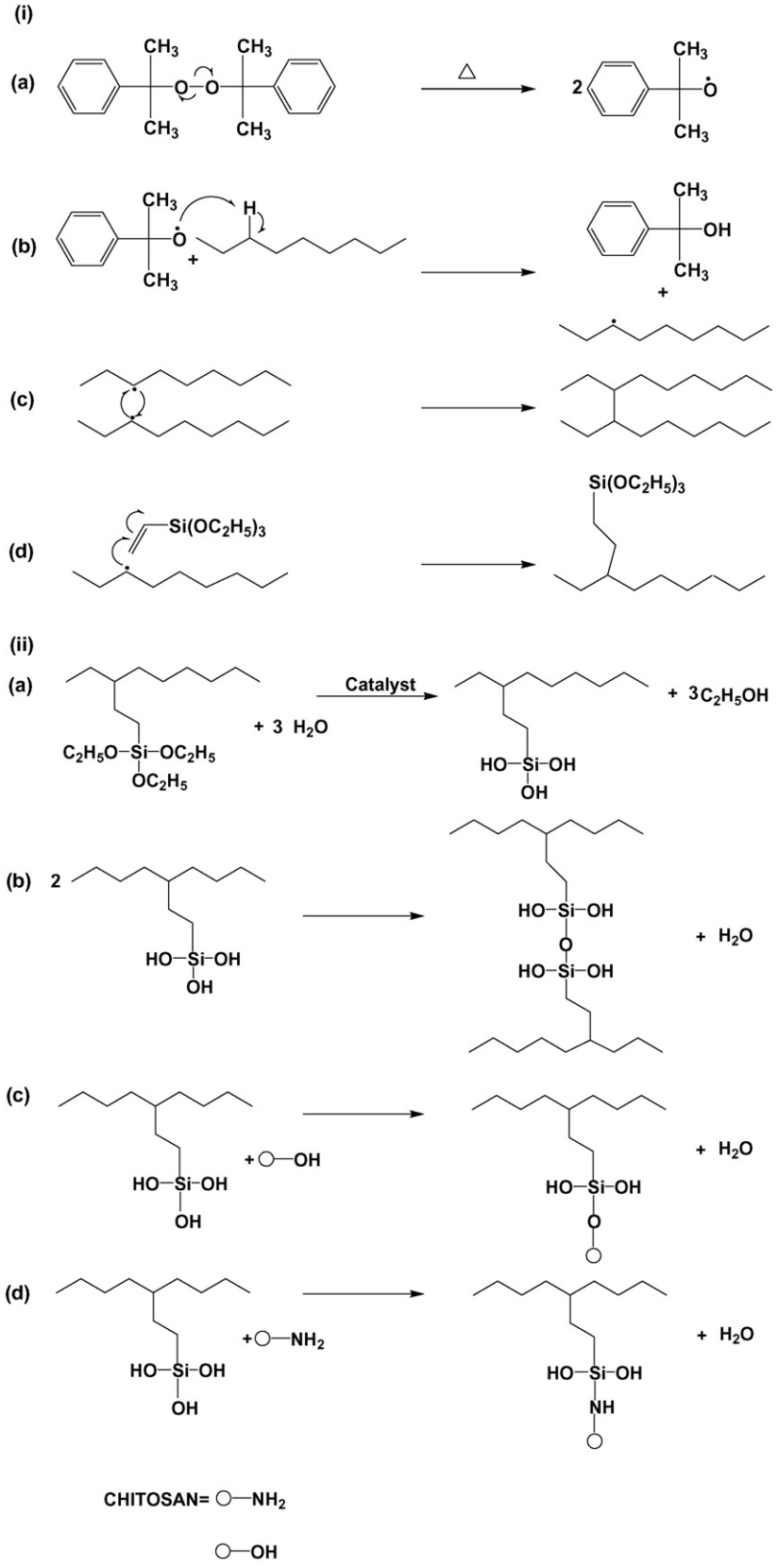

Scheme 1. (i) Reaction during processing, generation of free radicals from DCP (a), abstraction of hydrogen from polymer chain (b), crosslinking (c) and grafting reactions (d). (ii) Reaction during crosslinking, hydrolysis (a), self-condensation of silanol groups (b), condensation of silanol with hydroxyl group (c) and with amino group of chitosan (d).

Table 1
DSC and gel content analysis of HDPE/chitosan blends.[a].

Sample	T_m (°C)	ΔH_f (J/g)	T_c (°C)	ΔH_c (J/g)	X_c (%)	Gel content (%)
HP	130.3	184.1	117.2	259	63.4	–
HP15	129.8	154.5	116.8	243	53.2	–
HP25	129.7	143.5	116.6	230	49.4	–
HP30	129.6	133.3	116.6	206	45.9	–
HP35	129.6	131.1	116.5	201	45.2	–
XHP	129.8	179.1	116.6	257	61.7	9.2
XHP15	129.4	149.7	116.5	221	51.6	12.7
XHP25	128.9	139.2	116.4	203	48.0	21.0
XHP30	129.3	125.3	116.4	200	43.2	28.1
XHP35	129.0	114.1	116.3	191	39.3	40.0

[a] Prefix 'X' is used for crosslinked HDPE/chitosan blends.

polymer chains. An attack by the peroxy radicals on the double bond of the VTES was responsible for the grafting of VTES on polymer backbone. Radical induced crosslinking of blended materials has also occurred during processing. Silane crosslinking with various condensable groups were carried out in hot water as shown in Scheme 1 [ii (a–d)]. The first step during crosslinking was hydrolysis of silanol groups. The second step involved a number of reactions such as self-condensation of silanol groups and condensation reactions of silanol with hydroxyl and amino groups of chitosan (Nadia, Tariq, & Zareen, 2008). The presence of these reactions was confirmed by FTIR.

3.2. Particle size distribution

The particle size, distribution and dispersion of chitosan in the blend are important factors that affect the mechanical properties. The particle size distribution varied from 0.02 μm to 2000 μm. The mean percentage of particle size was found to be in the range of 441 μm. The particle size greater than 20 μm and less than 100 μm contributes 10% by volume while the particle size greater than 1000 μm contributes only 16% by volume.

3.3. Structural analysis

FTIR spectra of HP, HP25 and XHP25 are shown in Fig. 1. The important peaks of chitosan were present both in spectrum (b) and (c). The absorption peaks of chitosan at 1577 cm^{-1}, 1612 cm^{-1}, and 3284 cm^{-1} were assigned to N–H, C–O and O–H groups of chitosan respectively. In spectrum (c) the characteristic absorption band of polysiloxane (Si–O–Si) appeared at 1020 cm^{-1} and 1045 cm^{-1} (Hernandez, Rojas, Garcia, Canseco, & Castano, 2003; Magnus & Kristiina, 2006; Zhengzhou, Yuan, Zhou, & Ruowen, 2003). The peak at 1105 cm^{-1} was assigned to Si–O–C which was attributed to the covalent bonding between polymer and silane (Zakirov, Khabibullaev, & Chi, 2009). This absorption peak provided strong evidence about the crosslinking reaction. Additionally some peaks corresponded to (Si–O–Si) symmetric vibration were also observed at 805 cm^{-1} (Hernandez et al., 2003; Magnus & Kristiina, 2006). These peaks were absent in the spectrum of HDPE and non-crosslinked HP25.

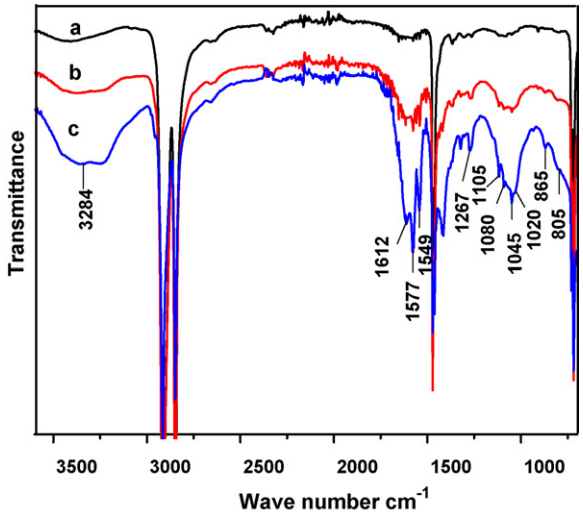

Fig. 1. IR spectra of HP (a), HP25 (b) and XHP25 (c).

3.4. Gel content

The gel contents of crosslinked samples are shown in Table 1. This table shows that the lowest gel content was observed for XHP and its quantity increased as the amount of chitosan increased in the blend. The maximum value of 40% gel content was observed for XHP35. The increasing tendency of gel content with increasing amount of chitosan was associated to the crosslinking reaction of silanol groups with hydroxyl and amino functionality of chitosan as shown in Scheme 1 [ii (c and d)]. At higher chitosan loading the probability of these reactions increased. Thus gel contents of these blends were found to be directly proportional to the amount of chitosan.

3.5. Thermogravimetric analysis

Fig. 2 shows weight loss of blended material against temperature. The virgin sample showed single stage degradation in the

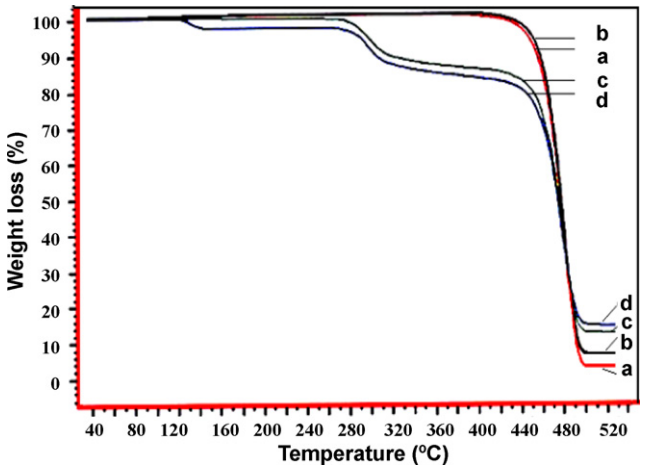

Fig. 2. TGA curves of HP (a), XHP (b), HP35 (c) and XHP35 (d).

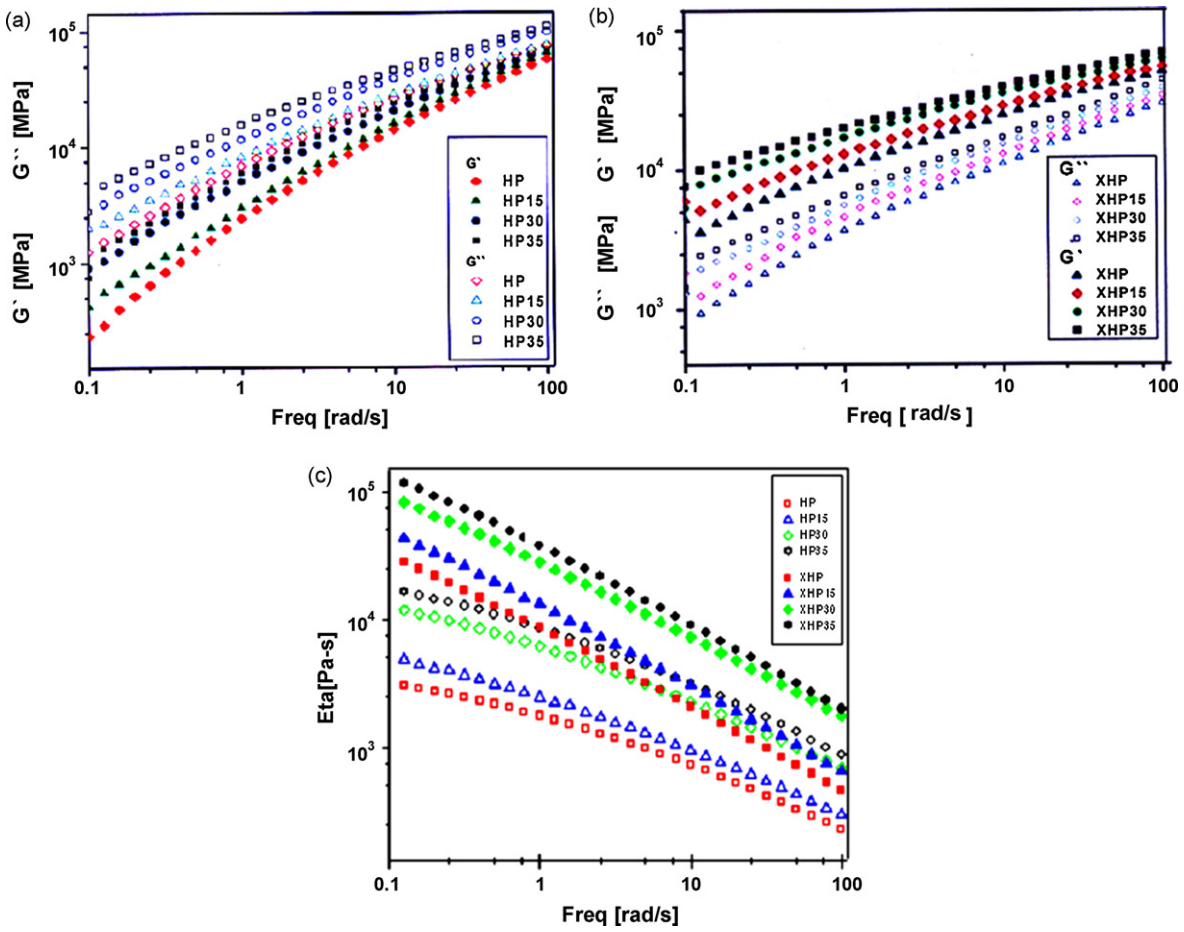

Fig. 3. Dynamic shear moduli (G' and G'') of non-crosslinked blends (a), crosslinked blends (b) and complex viscosities of non-crosslinked and crosslinked blends (c).

range of 420–500 °C corresponding to the decomposition of PE matrix, whereas crosslinking of HDPE with silane (XHP) resulted in higher thermal stability. The thermograms of non-crosslinked HDPE/chitosan blend showed two stages of degradation. The first stage ranging from 260 °C to 420 °C was due to thermal degradation of chitosan. In this stage, degradation of chitosan took place which involved dehydration, ring scission and decomposition reactions (Nadia et al., 2008). The second stage (420–500 °C) was attributed to the decomposition of PE matrix as observed in case of HP. The crosslinked HDPE/chitosan blends showed three stages in thermogram. The first stage ranging from 90 °C to 160 °C was due to water evaporation because the composites were crosslinked in hot water. The absence of first stage in non-crosslinked samples was mainly because these samples were not placed in hot water and the used chitosan was completely dried. The second and third stages were similar to non-crosslinked HDPE/chitosan blend.

It was also noted that increasing percentage of chitosan in HDPE/chitosan blends gave higher percentage of residue. The residue of HP35 was 14% while that of HP30 was 12%. Similar behavior was also observed for crosslinked formulations. The percentage of residue of crosslinked samples was higher than non-crosslinked formulations i.e. HP has 3% residue while XHP has 6%. DTA thermogram showed similar degradation pattern as that of TGA curves.

3.6. Differential scanning calorimetry

Table 1 presents melting temperature (T_m), crystallization temperature (T_c), heat of crystallization (ΔH_c), heat of fusion (ΔH_f) and the percentage crystallinity (X_c) of the samples. The crystallinity of silane crosslinked formulations was determined by the following equation:

$$X_c = \frac{\Delta H_f}{\Delta H_f^\circ} \times 100$$

where ΔH_f is the observed heat of fusion of the sample and ΔH_f° is the heat of fusion of 100% crystalline HDPE and was taken to be 290 J/g (Sirisin & Meksawat, 2004). The virgin HP has T_m 130.3 °C with X_c 63.4% whereas XHP has T_m 128.8 °C with X_c 61.7%. A small difference among the values of T_m and T_c was observed in both non-crosslinked and crosslinked blends but the percentage crystallinity was greatly affected by the incorporation of chitosan. It shows that chitosan inhibits the close packing of the PE chains. The X_c of HP15 and HP35 were 53.2% and 45.2% while those of XHP15 and XHP35 were 51.6 and 39.3%. The lower crystallinity of crosslinked formulations over non-crosslinked formulations was due to the formation of network structure (Jiao, Wang, Liang, & Hu, 2005). The network structure reduced the chain flexibility which lowered the peak crystallization temperature and consequently reduced crystallinity. Similar trend has been reported for in thermoplastic wood composite (Magnus & Kristiina, 2006).

3.7. Rheological analysis

Melt rheology of thermoplastic blends is vital to understand the structural property relationship and their processibility. The presence of stable viscoelastic region was confirmed by time and strain sweep experiment before the frequency sweep. The results show

Table 2
Tensile properties of non-crosslinked and crosslinked blends.

Sample	TS (MPa)	Eb (%)	Sample	TS (MPa)	Eb (%)
HP	8.1 ± 1.0	403.3 ± 9.2	XHP	9.3 ± 0.5	336.9 ± 7.3
HP15	7.6 ± 1.3	18.1 ± 1.0	XHP15	14.4 ± 1.5	21.4 ± 2.5
HP30	5.7 ± 0.7	8.0 ± 0.5	XHP30	25.7 ± 1.7	9.3 ± 1.3
HP35	5.6 ± 0.5	7.3 ± 0.5	XHP35	27.4 ± 2.9	7.3 ± 1.8

that both the non-crosslinked and the crosslinked samples were within the linear viscoelastic region.

Fig. 3a and b shows the dynamic shear moduli of non-crosslinked and crosslinked formulations at 150 °C and the complex viscosities (η^*) of these formulations are shown in Fig. 3c. It can be seen from Fig. 3 that both the composition and crosslinking in the blend affected the values of G', G'' and η^*. These variation in G' and G'' corresponded to energy change occurring during dynamic shear process and are strongly dependent on interaction between polymers interphase in the blend (Rhon, 1995).

An increase in G' and G'' values with increase in frequency was observed for both non-crosslinked and crosslinked formulations. This is due to the fact that at low frequency, time is large enough to unfold the chains and they relax slowly. This high relaxation tends to reduce the G' and G'' values. However when polymer chains were deformed at higher frequency, the entangled chain had less time for re-orientation which increased the moduli. Similar behavior was also reported for the compatibilized low density polyethylene and ethylene octane copolymer blend (Baghaei et al., 2009).

Fig. 3a also revealed that in case of non-crosslinked formulation the G'' curves were well above the G' curves. This shows that chitosan has a poor interaction with HDPE and the components were weakly associated with each other. As chitosan is hydrophilic and polyethylene is hydrophobic in nature, therefore, the resultant blend of these two components was immiscible. It was also observed that G'' values of non-crosslinked formulations increased linearly with increasing percentage of chitosan.

In Fig. 3b, the crosslinked blend shows opposite behavior to that of non-crosslinked blend i.e. the G' curves were higher than G''. This showed that a strong interaction was developed between the polymers interphase by VTES. The silane forms a network structure between the HDPE–chitosan interphase which enhances the elastic properties of these materials.

Fig. 3c depicts complex viscosities of non-crosslinked and crosslinked formulations. This figure shows that complex viscosity (η^*) increased with increasing chitosan amount in the blend and decreased with increasing frequency. This was due to the strong shear thinning behavior of the blend at molten state (Baghaei et al., 2009). The silane crosslinked formulations have higher η^* than non-crosslinking formulations. This behavior might be due to the formation of network structure formed by VTES which causes greater resistance under shear flow. Besides this, the amount of chitosan loading also increased the η^* of both types of formulations. In non-crosslinked formulations, greater amount of chitosan loading will cause greater entanglement of the chains and thus gradually increases the η^*.

3.8. Tensile properties

The tensile properties of HDPE/chitosan blends are shown in Table 2. This table illustrates that the tensile strength (TS) of crosslinked samples was much higher than non-crosslinked samples. The TS showed direct relationship with gel content of crosslinked blends. The TS of virgin HP was 8 MPa and it increased by 16% to 9.31 MPa in XHP. Similarly the XHP15 (14.4 MPa) showed twofold enhancement as compared to HP15 (7.6 MPa). The maximum TS was observed for XHP35 (27.4 MPa) which was 5 times higher than HP35 (5.6 MPa). The increasing trend in tensile properties was attributed to the strong interaction developed between the polymer interphase. Both the non-crosslinked and crosslinked samples showed poor elongation properties but the effect was more pronounced in the non-crosslinked formulations. The maximum value of percentage elongation (Eb) was seen in XHP15 which was 21% whereas HP15 showed 18%. The Eb values decreased with increased chitosan amount in the blend and lowest Eb values were observed in HP35 and XHP35. Similar behavior was observed by other authors in similar system (Balsuriya, Ye, Yiu, & Wu, 2005; Byung & Soo, 2001).

3.9. Creep test

Creep study was carried out by using dynamic mechanical thermal analyzer and the results are shown in Fig. 4. In this figure highest deformation was observed for neat HP as compared to XHP. The addition of chitosan in HDPE lowered the deformation and it decreased further with increasing amount of chitosan in HDPE/chitosan blends. The non-crosslinked blends showed greater deformation as compared to their corresponding crosslinked blends. The XHP35 showed less deformation than HP35. The lower deformation in the crosslinked blends was associated to silane crosslinking which holds the macromolecular chain firmly whereas in non-crosslinked samples, the molecular chain moved freely and the hydrophobic–hydrophilic repulsion of HDPE and chitosan further facilitated this phenomenon.

3.10. SEM analysis

Fig. 5a and b shows scanning electron micrograph's of the fractured surfaces of HP35 and XHP35 formulations. Micrographs of the non-crosslinked blend show clear chitosan particles, which were loosely embedded in polyethylene matrix. Various gaps were observed between the HDPE and chitosan interphase. This shows

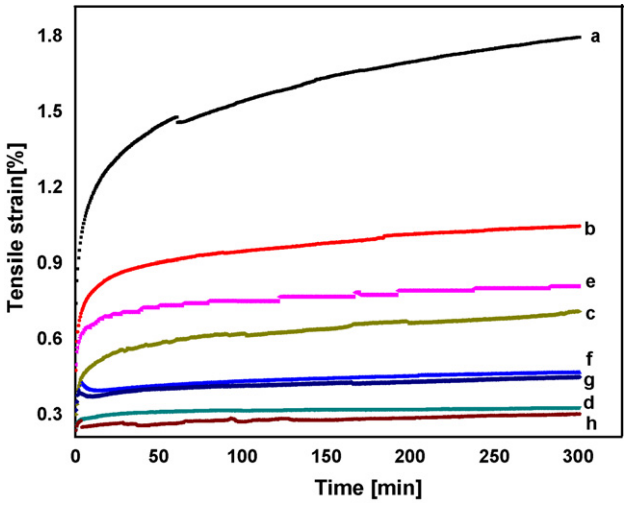

Fig. 4. Creep analysis of non-crosslinked samples [HP (a), HP15 (b), HP25 (c), HP35 (d)] and crosslinked samples [XHP (e), XHP15 (f), XHP25 (g) and XHP35 (h)].

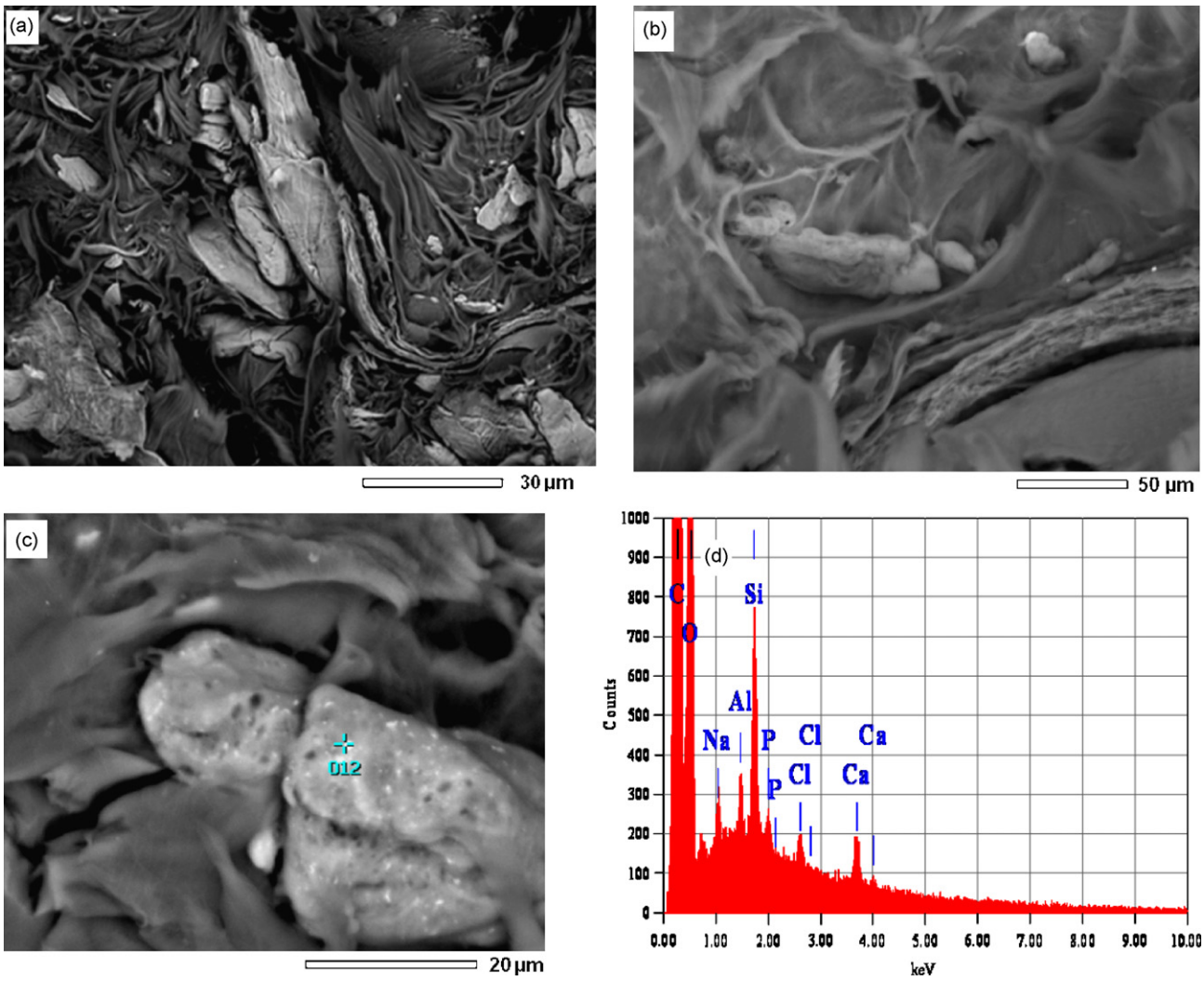

Fig. 5. Scanning electron micrograph of non-crosslinked blend HP35 (a), scanning electron micrograph of crosslinked blend XHP35 (b), EDS micrograph of the crosslinked blend XHP35 (c) and EDS spectrum of the crosslinked blend XHP35 (d).

poor adhesion between HDPE and chitosan. This was the main cause of lower mechanical properties of these blends. Whereas crosslinked blend (XHP35) showed better adhesion between chitosan and HDPE. As VTES improves the miscibility of HDPE and chitosan, consequently HDPE seems to adhere the chitosan particle very well.

Fig. 5c and d show elemental analysis results of XHP35 obtained by EDS technique. In Fig. 5a the marked region of chitosan particles showed some characteristic elemental peaks. The presence of silicon peak gives evidence about the crosslinking reaction between chitosan and polyethylene matrix. Some peaks corresponding to sodium, calcium and aluminum were also obtained which might be due to the remains of impurities and/or catalyst etc. present in the polymer resin.

4. Conclusions

HDPE/chitosan blends were prepared by a peroxide-initiated melt compounding technique and VTES was used as crosslinker. The crosslinked blends showed distinct absorption peaks of Si–O–C and Si–O–Si at 1105 cm^{-1} and 1020 cm^{-1} which confirmed the crosslinking reaction. The degree of crosslinking was found to be directly proportional to the amount of chitosan at fixed VTES amount. Thermogravimetric analysis of the non-crosslinked and crosslinked HDPE/chitosan blends showed two and three stage degradation behavior respectively. It was also noted that increasing percentage of chitosan in the blends gave higher percentage of residue. Differential scanning calorimetry showed decreasing trend of percentage crystallinity and peak melting temperature with increasing amount of chitosan which was associated to the formation of network structure and the disorder of close packing of polyethylene chains. The minimum percentage crystallinity was observed for XHP35. Dynamic melt rheological behaviour of the blends was within linear viscoelastic region. The complex viscosity and dynamic shear storage modulus (G') of the crosslinked samples were well above the non-crosslinked samples which showed a strong interaction between the matrix–filler interphase and the elastic nature of the crosslinked blend. High tensile strength was observed for the crosslinked samples and increases with increasing amount of chitosan in the blend. Tensile strength of crosslinked HDPE/chitosan blends containing 35% chitosan contents was 27.4 MPa which was three time higher than the XHP. Results of creep experiment indicated small deformation in crosslinked blends which showed that silane crosslinking effectively linked the two immiscible components. Similarly scanning electron microscopy also confirmed good compatibility and strong adhesion between HDPE and chitosan interphase.

Acknowledgements

Mr. Sadullah Mir wishes to thank Higher Education Commission of Pakistan for financial assistance and the Center for High Performance Polymer, University of Queensland, Australia for technical support.

References

Alain, B., & Sylvie, P. (2008). Investigations on mechanical properties of poly (propylene) and poly (lactic acid) reinforced by miscanthus fibers. *Applied Science and Manufacturing*, *4*, 1444–1454.

Araujo, J. R., Waldman, W. R., & De Paoli, M. A. (2008). Thermal properties of high density polyethylene composites with natural fibres coupling agent effect. *Polymer Degradation and Stability*, *93*, 1770–1775.

Baghaei, B., Jafari, S. H., Khonakdar, H. A., Rezaeian, I., Ashabi, L., & Ahmadian, S. (2009). Interfacially compatibilized LDPE/POE blends reinforced with nanoclay, investigation of morphology, rheology and dynamic mechanical properties. *Polymer Bulletin*, *62*, 255–270.

Balsuriya, P. W., Ye, L., Yiu, W. M., & Wu, J. (2005). Mechanical properties of wood flake polyethylene composite. II. Interface modification. *Journal of Applied Polymer Science*, *83*, 2505–2521.

Byung, C. J., & Soo, Y. H. (2001). Mechanical properties and morphology of the modified HDPE/starch reactive blend. *Journal of Applied Polymer Science*, *82*, 3313–3320.

Constance, R., Chu, A. Z., & Monosov, D. A. (1995). In situ assessment of cell viability within biodegradable polylactic acid polymer matrices. *Biomaterials*, *16*, 1381–1384.

Girones, J., Pimenta, M. T. B., Vilaseca, F., de Carvalho, A. J. F., Mutje, P., & Curvelo, A. S. (2007). Blocked isocyanates as coupling agents for cellulose-based composites. *Carbohydrate Polymers*, *68*, 537–543.

Hernandez, P. G., Rojas, F., Garcia, G. M., Canseco, M. A., & Castano, M. (2003). Development of hybrid materials consisting of SiO_2 microparticles embedded in phenolic–formaldehydic resin polymer matrices. *Materials Science and Engineering A*, *5*, 338–347.

Hongdian, L., Yuan, H., Ming, L., Zuyao, C., & Weicheng, F. (2006). Structure characteristics and thermal properties of silane-grafted-polyethylene/clay nanocomposite prepared by reactive extrusion. *Composites Science and Technology*, *66*, 3035–3039.

Jiao, C., Wang, Z., Liang, X., & Hu, Y. (2005). Non-isothermal crystallization kinetics of silane crosslinked polyethylene. *Polymer Testing*, *24*, 71–80.

Jung, K. P., & Junseok, Y. (2009). Guided bone regeneration by poly(lactic-co-glycolic acid) grafted hyaluronic acid bi-layer films for periodontal barrier applications. *Acta Biomaterialia*, *5*, 3394–3403.

Magnus, B., & Kristiina, O. (2006). The use of silane technology in crosslinking polyethylene/wood flour composites. *Applied Science and Manufacturing*, *7*, 52–765.

Magnus, B., Paul, G., & Kristiina, O. (2005). The effect of crosslinking on the properties of polyethylene/wood flour composites. *Composites Science and Technology*, *65*, 1468–1479.

Maria, R., Mariola, J., & Helena, J. (1998). Biodegradation of polycaprolactone in sea water. *Reactive and Functional Polymers*, *38*, 27–30.

Nadia, R., Tariq, Y., & Zareen, A. (2008). Synthesis of CM-chitosan/acrylic acid hydrogels using silane crosslink. *e-Polymers*, *142*.

Orhan, Y., Hrenovic, J., & Buyukgungor, H. (2004). Biodegradation of plastic compost bags under controlled soil conditions. *Acta Chimica Slovenica*, *51*, 579–588.

Otey, F. H., Westhoff, R. P., & Doane, W. M. (1980). Biodegradable starch-based blown films, industrial and engineering chemistry products. *Research and Development*, *19*, 592–595.

Rhon, Ch. L. (1995). *Analytical polymer rheology*. Cincinnati, OH: Hanser/Gardener Publications Inc.

Sekiguchi, S. (1994). Molecular weight dependency of antimicrobial activity by chitosan oligomers. In *Food hydrocolloids: structures, properties, and functions*. New York, USA, pp. 71–76.

Sirisin, K., & Meksawat, D. (2004). Comparison in processability and mechanical and thermal properties of ethylene–octene copolymer crosslinked by different techniques. *Journal of Applied Polymer Science*, *93*, 1179–1185.

Tae, I. M., & Hiroshi, I. (1980). New aspects of graft copolymerization of styrene onto cellulose induced by gamma rays. *Polymer*, *21*, 309–316.

Tzankova, D. N., & Lamantia, F. P. (1999). Recycling of the light fraction from municipal post-consumer plastics effect of adding wood fibers. *Polymers for Advanced Technologies*, *10*, 607–614.

Valenza, A., Visco, A. M., & Acierno, D. (2002). Characterization of blends with polyamide 6 and ethylene acrylic acid copolymers at different acrylic acid content. *Polymer Testing*, *21*, 101–109.

Zakirov, A. S., Khabibullaev, P. K., & Chi, K. Y. (2009). Structural characterization and electro-physical properties for SiOC (H) low-k dielectric films. *Journal of Physics B*, *08*, 260–269.

Zhengzhou, W., Yuan, H., Zhou, G., & Ruowen, Z. (2003). Halogen free flame retardation and silane crosslinking of polyethylenes. *Polymer Testing*, *22*, 533–538.

Zivanovic, S. P., Li, J., Davidson, M., & Kit, K. (2007). Physical mechanical, and antibacterial properties of chitosan/PEO blend films. *Biomacromolecules*, *8*, 1505–1510.